CFD calculations of gas leak dispersion and subsequent gas explosions: Validation against ignited impinging hydrogen jet experiments

Prankul Middha [a,*], Olav R. Hansen [a], Joachim Grune [b], Alexei Kotchourko [c]

[a] GexCon A.S., P.O. Box 6015, Postterminalen, NO-5892, Bergen, Norway
[b] ProScience, Karlsruhe, Germany
[c] Forschungszentrum Karlsruhe GmbH, 76344 Eggenstein-Leopoldshafen, Germany

ARTICLE INFO

ABSTRACT

Computational fluid dynamics (CFD) tools are increasingly employed for quantifying incident consequences in quantitative risk analysis (QRA) calculations in the process industry. However, these tools must be validated against representative experimental data, involving combined release and ignition scenarios, in order to have a real predictive capability. Forschungszentrum Karlsruhe (FZK) has recently carried out experiments involving vertically upwards hydrogen releases with different release rates and velocities impinging on a plate in two different geometrical configurations. The dispersed cloud was subsequently ignited and resulting explosion overpressures recorded. Blind CFD simulations were carried out prior to the experiments to predict the results. The simulated gas concentrations are found to correlate reasonably well with observations. The overpressures subsequent to ignition obtained in the blind predictions could not be compared directly as the ignition points chosen in the experiments were somewhat different from those used in the blind simulations, but the pressure levels were similar. Simulations carried out subsequently with the same ignition position as those in the experiments compared reasonably well with the observations. This agreement points to the ability of the CFD tool FLACS to model such complex scenarios even with hydrogen as a fuel. Nevertheless, the experimental set-up can be considered to be small-scale. Future large-scale data of this type will be valuable to confirm ability to predict large-scale accident scenarios.

© 2010 Elsevier B.V. All rights reserved.

1. Introduction

Computational fluid dynamics (CFD) calculations are being used more and more to perform quantitative risk assessments in recent years, especially in the oil and gas industry. These tools provide the possibility to directly model the physics of phenomena that are relevant to process safety such as gas dispersion and explosion. Based on predicted consequences of a range of potential accident scenarios a risk level is estimated. However, we need to be careful before applying a CFD tool to carry out such risk assessments. The tool needs to be well validated against a range of relevant experiments in order to have real predictive capability (with studies on variations of various important parameters that may affect explosion loads and hence risk). Nonetheless, when CFD consequence prediction tools are validated, there is a significant focus on basic situations, like free jet releases for dispersion, or pre-mixed homogeneous gas mixtures for explosions. It must be pointed out

that the typical accident scenario is usually more complicated, possibly involving time varying releases impinging on equipment, with delayed ignition of a non-homogenous and possibly turbulent mixture. When aiming for increased precision in risk assessment methods there is a need to validate consequence tools for this added complexity. For post-accident simulations, it is obvious that there is a need to reproduce the complex physics of the accident scenario, and validation of tools for the combined release and ignition scenarios is important. For the modelling of such a situation, validation or verification against idealized scenarios is far from sufficient. A very important cause of this gap in "real" validation of CFD tools is that it is challenging to perform good experiments with such a complexity. Good experimental data involving scenarios reminiscent of those seen in real situations are few and far between, especially at large scales. Even for hydrocarbons, there are only a very few such experiments available, the most notable being the Phase3B experiments carried out at Spadeadam test site in north-west England.

Over the past few years, the focus on carrying out safety studies for hydrogen applications has increased. This is primarily due to the fact that the possibility of using hydrogen as an energy carrier has increasingly caught interest of both public and government policy makers in recent times. There has also been increasing attention

from the nuclear industry. Further, the hazards of hydrogen are well known and it is important to demonstrate that the expected large-scale use of hydrogen in the future does not increase the risk to society. The use of CFD for this purpose has also become more frequent. However, the CFD tool needs to be well validated against relevant experiments. With these considerations, a strong effort has been made in the past few years to learn more about hydrogen explosions and improve FLACS in that area. We have carried out dedicated research projects involving varied small-scale experiments, combined with simulations and model improvements in order to improve the validation database for hydrogen safety predictions [1]. Simulations of many large-scale experiments from various external sources have also been carried out. This includes explosion simulations for Sandia FLAME facility [1], Fh-ICT 20 m hemispherical balloon [2], SRI confined tube [3], Fh-ICT lane experiments [4], McGill detonation tubes [5], and more. Dispersion simulations have been carried out to validate predictive capabilities for sonic jets [6] (e.g. HSL tests, INERIS experiments, and FZK tests) and subsonic jets (INERIS garage experiments [7], Swain experiments [6], GexCon low momentum release experiments [8]). A summary of the validation efforts for FLACS simulations for hydrogen deflagrations has recently been published [9].

However, none of the experiments used for validation involved simultaneous dispersion and ignition. For this reason, experiments carried out by Forschungszentrum Karlsruhe (FZK) as a part of the internal project InsHyde of the EU-sponsored Network of Excellence (NoE) HySafe (http://www.hysafe.org) were adopted for validation in the present work. These experiments have supported the development of approaches for quantitative risk analysis (QRA) studies for hydrogen applications [10]. This is because this type of experiments provides a possibility to validate important assumptions used in probabilistic quantitative risk assessments, which are necessary to limit number of scenarios studied (e.g. equivalent stoichiometric cloud size methods). Such calculations are performed and are presented in the following sections.

Nevertheless, the experimental set-up can be considered to be small-scale and consequences can be expected to be less severe than many accidents and real-life situations. Future large-scale data of this type will be valuable to confirm ability to predict large-scale accident scenarios.

2. Brief description of experiments

This study involved vertically upwards hydrogen releases (upto 10 g hydrogen released through one of three different nozzles with release time of 0.1–100 s) impinging on a horizontal plate or hood (plate with side walls). After a time delay, the dispersed cloud was ignited and pressures recorded. The experiment is a hydrogen
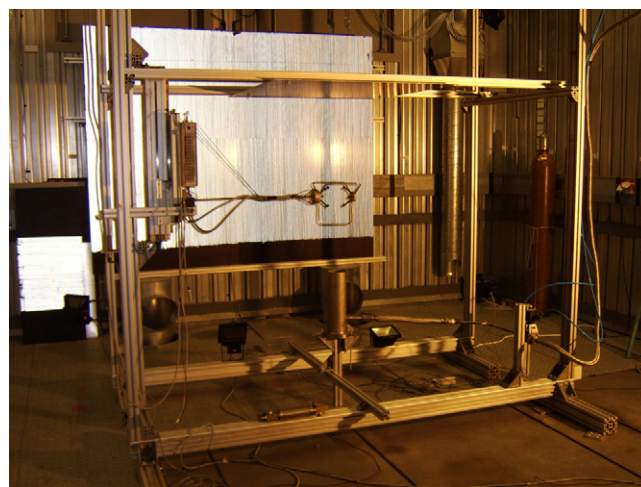

Fig. 1. A photograph of the experimental set-up.

release scenario with subsequent ignition in an almost open geometry. Two different geometrical configurations were considered in the experiments:

1. Square horizontal plate (dimension 1.0 m) at a distance of 1.50 m above the release nozzle.
2. Same set-up as configuration 1 but with four additional vertical sidewalls of 0.50 m height, forming a downward open hood with a volume of 500 L above the release nozzle.

A photograph of the experimental set-up for the plate only geometry is shown in Fig. 1. A schematic view of the two configurations is presented in Fig. 2.

Nine hydrogen release scenarios were investigated in the experiments, covering three different diameters of the circular release nozzle (100, 21, and 4 mm) with three different constant hydrogen release rates each. These scenarios are summarized in Table 1, along with the corresponding exit velocities and the total release time. It should be pointed out that the total hydrogen inventory was fixed at 10 g in all cases.

Hydrogen concentrations between the nozzle and plate were determined by collecting gas samples in eight cylinders. Since a stable plume needs some time to establish above the release, measurements were performed at times close to the end of the duration of the hydrogen release. The hydrogen content of the sample taking cylinders was determined using a gas analysis system (Fisher-Rosemount, Series MLT) with a measuring range from 0 to 100 vol.%
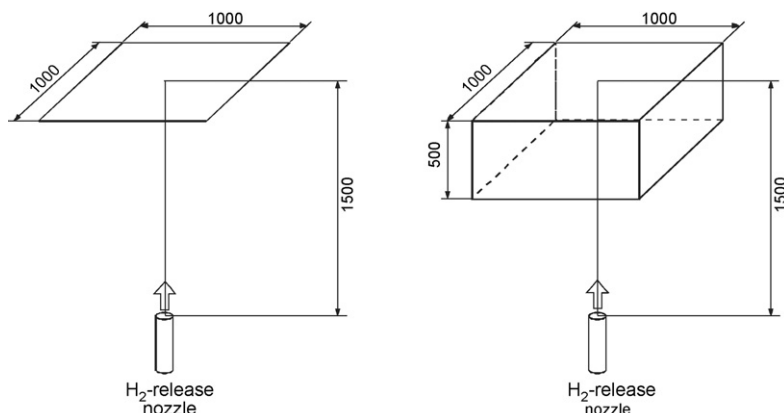

Fig. 2. Configurations investigated in the experiments: (left) configuration 1 (horizontal plate), (right): configuration 2 (horizontal plate with sidewalls).

Table 1
Release scenarios investigated in the experiments.

Experimental series	Nozzle diameter [mm]	Exit velocity [m/s]	Mass flow [g/s]	Release duration for 10 g H_2 inventory [s]
A	100	0.2	0.14	71.3
B	100	1	0.7	14.3
C	100	5	3.5	2.85
D	21	5	0.15	64.7
E	21	100	3	3.23
F	21	200	6	1.62
G	4	100	0.14	70
H	4	200	0.29	35
I	4	400	0.57	17.5

H_2 and 0–100 vol.% O_2. The concentration measurements were also used to determine appropriate positions for the ignition source in the subsequent combustion experiments.

The released hydrogen was ignited using a high frequency spark at two different ignition positions (0.8 and 1.2 m above the release nozzle). Combustion overpressure measurements were performed using ten piezoelectric pressure gauges (PCB, Models 112A21, 113A21 and 113A31). Eight of these sensors were fixed to a bar in a distance of 20 cm to each other (starting at 0.25 m above the release). The two remaining pressure transducers were installed to the same bar at locations in between these positions. The whole bar was then installed vertically at a distance of 0.4 m to the axis of the hydrogen release. More details of the experiments can be found in reference [11].

3. Simulation details

In the weeks prior to the planned experiments, we performed several blind CFD simulations to predict the outcome of the proposed experiments, and if possible, to help the planning. After the experiments were reported, the quality of the blind predictions was evaluated. The gas concentrations of the impinging jets were generally well predicted, both along and across the jet. The explosion experiments were performed with a slightly different ignition position than the blind predictions, but still the predicted pressure level was representative of the observations. Simulations with the exact ignition positions of the experiments were performed after the tests, and confirmed the ability of the CFD tool FLACS to predict the pressures from ignition of non-homogeneous hydrogen clouds.

All the simulations have been carried out using the CFD tool FLACS. FLACS is a CFD tool that solves the compressible Navier–Stokes equations on a 3-D Cartesian grid. The tool is used extensively for simulating problems relevant to process safety. It has specifically been designed for modelling the consequences of a flammable gas release in a semi-confined region. The software consists of a pre-processing module (CASD) that is used to build 3D models for complex geometries and define the simulation grid and scenario parameters. Due to the use of a distributed porosity concept, FLACS can therefore be used to simulate most kinds of complicated geometries using a Cartesian grid (see below). A good description of geometry and the coupling of geometry to the flow, turbulence, and flame is one of the key elements in the modelling. The core simulator includes conservation equations for mass, momentum, enthalpy, mass fraction of chemical species, turbulent kinetic energy, and dissipation rate of turbulent kinetic energy. The SIMPLE method for pressure correction is used [12]. FLACS uses a standard k–ε model for turbulence with some modifications including a model for generation of turbulence behind sub-grid objects and turbulent wall functions [13]. The post-processing module Flowvis can be used to convert the calculation results (in terms

of several physical variables) into scalar-time curves, 2D contour plots, 3D plots, or volume plots in a static/dynamic form as required. Several explosion experiments used to develop and validate FLACS have been published [14–16]. In addition, a number of validation reports and more details about the software are available at GexCon's web pages [17,18].

FLACS contains a combustion model that assumes that the flame in an explosion can be regarded as a collection of flamelets. One-step reaction kinetics is assumed, with the laminar burning velocity being a measure of the reactivity of a given mixture. A chemical equilibrium model is used to estimate the composition of the combustion products. These include H_2O and CO_2, but also increasing amounts of H_2, CO and OH for rich concentrations and high temperatures. Heat is added due to combustion and the heat capacities for different gases depend strongly on temperature. The model consists of two parts: a three-step burning velocity model and a flame model. To represent flame folding around sub-grid obstacles, a flame folding model has also been implemented. The flame model gives the flame a constant flame thickness (equal to 3–5 grid cells) and assures that the flame propagates into the reactant with the specified velocity that is based on a series of parameters. The flame is propagated based on the transport of "products" into new cells and subsequently "burns" with a specified velocity as indicated above. A number of correction models are made to compensate for weaknesses due to flame thickness, e.g. flame folding behind sub-grid objects which ensure good results for a range of grid resolutions. The real flame area is properly described. For a finite thickness of the reaction zone (3–5 grid cells), the flame area needs to be corrected for curvature at these scales and smaller. All flame wrinkling at scales less than the grid size must be represented by sub-grid models (and this is important for flame interaction with objects of the grid size or less).

The burning velocity model consists of the following three models: (a) a laminar burning velocity model that describes the laminar burning velocity as a function of gas mixture, concentration, temperature, pressure, oxygen concentration in air and amount of inert diluents, (b) a model describing quasi-laminar combustion in the first phases of flame propagation after ignition. Due to flame instabilities, the observed burning velocity increases as the flame propagates away from ignition (due to flame wrinkling). All flame wrinkling at scales less than the grid size is represented by sub-grid models, which is important for flame interaction with objects smaller than the grid size, and (c) a model that describes turbulent burning velocity as a function of turbulence parameters (intensity and length scale). The model is based on a broad range of experimental data reported in Abdel Gayed et al. [19]. Bray [20] found that the data from reference [19] could be represented in a reasonable manner by the following empirical expression:

$$\frac{S_T}{S_L} = 0.875 K^{-0.392} \frac{u'}{S_L}$$

where, K is the Karlovitz stretch factor, S_T is the turbulent burning velocity, and S_L is the laminar burning velocity. Corrections for Lewis number are also implemented.

The FLACS code uses a "distributed porosity concept" which enables the detailed representation of complex geometries using a relatively course Cartesian grid. Large objects and walls are represented on grid, and smaller objects are represented sub-grid. This enables geometrical details to be characterized while maintaining reasonable simulation times. This approach represents geometrical details as porosities (opposite of blockage) for each control volume. The porosity concept models the blockage, drag formulation, sub-grid turbulence generation and flame folding coefficients to obtain good simulation results despite coarse grid resolutions. Sub-grid objects contribute to flow resistance, turbulence generation and flame folding in the simulation as it is important to model the tur-
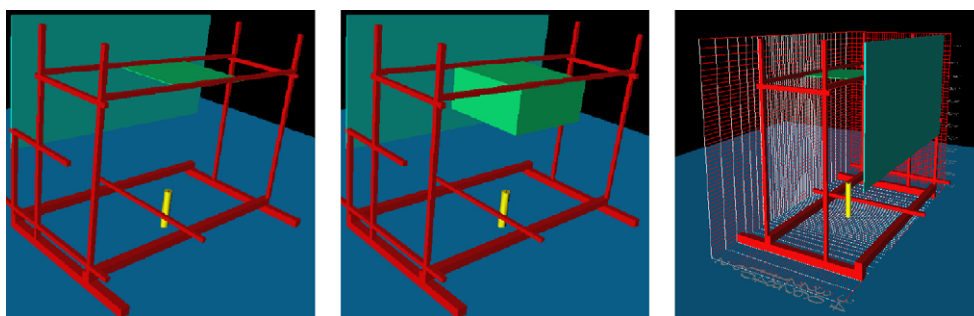
Fig. 3. Representation of the experimental geometry in FLACS. The grid applied is also presented.

bulence correctly for partly porous and "sub-grid" objects to obtain good results. In case of small objects, the flow kinetic energy lost due to drag is compensated as a source term for turbulent energy. The geometry representation has been optimized so that the dependency on grid size, shape, and translation is as low as possible. More details are given in [12,13].

All the scenarios described in the experimental set-up were simulated. The experimental geometry for the two different configurations as represented in FLACS is presented in Fig. 3. The computational grid used in the simulations for the dispersion calculations is also shown in the same figure for the case of a single plate for the 100 mm nozzle. Please note that similar grid resolution is used for the other geometries and scenarios with the same nozzle size. The grid was made coarser away from the orifice and the enclosing plates in order to improve computational efficiency. However, the grid was appropriately adjusted for the smaller nozzles, as finer grid resolution is required in the vicinity of the orifice to model the leaks properly. The explosion calculations are performed on a finer grid with 2.5 cm grid resolution in the interesting region. The refinement was necessary to comply with the grid guidelines for explosions, which require a certain number of grid cells across a gas cloud. The summary of the grid sizes is presented below in Table 2. A total of 30 measurement sensors were used in the simulations. All of them were placed in the plane $Y = 0$, with 10 each at $X = 0$, 0.2, and 0.4 m.

Simulation time on single CPUs vary from a couple of hours to a few days, depending on nozzle size, leak velocity and duration of leak. The release scenarios with a small nozzle and long release time are the most time consuming. The simulations were carried out in quiescent conditions with passive boundary conditions (no wind). For combustion simulations with real gas cloud, the dispersion results were dumped and the simulations were restarted with the appropriate explosion grid (equidistant in all directions) following the grid guidelines of the CFD program. The explosion calculations are performed on a finer grid with 2.5 cm grid resolution in the interesting region (see Table 2). The refinement was necessary to comply with the grid guidelines for explosions, which require a certain minimum number of grid cells across a gas cloud.

Several dispersion simulations and explosion calculations were carried out *blind* without any prior knowledge of experimental

Table 2
Summary of the grid resolution for all dispersion and explosion calculations.

Nozzle size	Normal grid resolution in interesting region (cm)	Grid resolution near the leak	Total grid cells
100 mm	5	5 cm	70,312
21 mm	5	2 cm	89,817
4 mm	5	0.5 cm	135,877
Explosion	2.5	N.A.	251,720

Table 3
Summary of all calculations (blind and post) described in this article.

Nozzle diameter	Geometry	Release rate (g/s)	Blind calculations	Post-calculations
100	Plate	0.14	✓	✓
		0.7	✓	✓
		3.5	✓	
	Hood	0.14	✓	✓
		0.7	✓	✓
		3.5	✓	
21	Plate	0.15	✓	✓
		3	✓	
		6	✓	
	Hood	0.15	✓	✓
		3	✓	
		6	✓	
100	Plate	0.14	✓	
		0.7	✓	✓
		3.5	✓	✓
	Hood	0.14	✓	
		0.7	✓	✓
		3.5	✓	✓
21	Plate	0.15	✓	
		3	✓	✓
		6	✓	✓
	Hood	0.15	✓	
		3	✓	✓
		6	✓	✓

data. However, post-calculations were carried out for low momentum releases where the grid resolution could be insufficient in the blind calculations. Post-calculations were also carried out for several explosion simulations where the ignition position used was inconsistent with the experiments. A summary of all the calculations (blind and post) described in the current article is presented in Table 3.

4. Results and discussion

This section presents selected results obtained during the experiments and comparisons with relevant simulation results. The results obtained in the dispersion study are presented first and the pressure loads subsequent to ignition of dispersed clouds are presented next. Detailed results of all the simulations that were performed, compared with experiments are available in reference [21].

4.1. Dispersion

The dispersion simulations showed that the sizes of the flammable gas clouds for the plate only geometry are generally insignificant. For the hood geometry, hydrogen gas was seen to accumulate between the sidewalls. This may contribute to a consid-
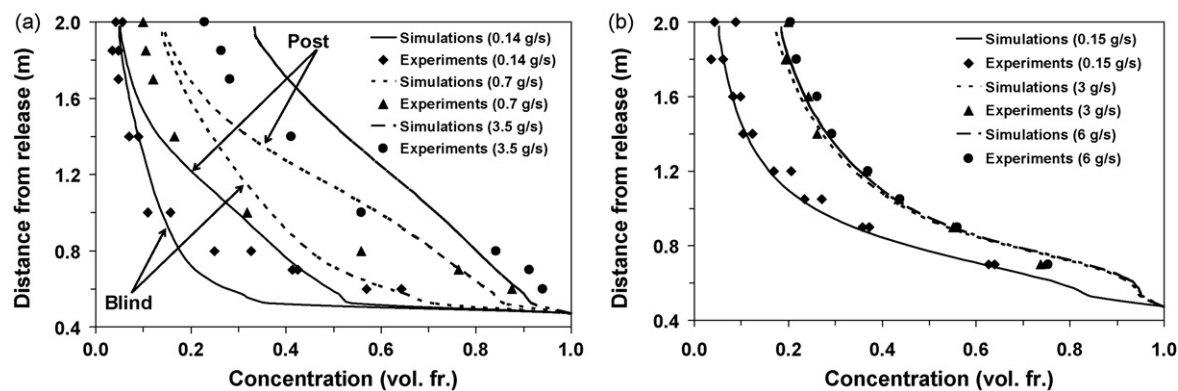
Fig. 4. Comparison of experimental concentration profiles and FLACS predicted concentration contours for releases from 100 mm (left) and 21 mm (right) nozzle (plate geometry).

erable overpressure upon ignition. Additional simulations carried out with the nozzle located 1.0 m below the plate revealed that the lower release position (1.5 m) led to somewhat larger flammable gas clouds. Also, the 4 mm nozzle failed to generate significant gas clouds for all six cases. This is likely due to the fact that the high momentum release is very quickly mixed and hence diluted to concentrations below the lower flammability limit (LFL).

In Fig. 4, concentration profiles from FLACS blind predictions for all three release rates for the 100 and 21 mm nozzles for the plate geometry are compared with experimental results. It should be noted that the release nozzle is located at a height of 0.5 m. A detailed comparison of simulated vs. reported profiles from experiments indicates that there is a reasonable correlation between predictions and experiments for the tests with 100 mm nozzle but some deviation can still be seen. In general, the simulation results for releases from the largest nozzle show an under-prediction near the release nozzle, and an over-prediction away from the release nozzle. The three 21 mm nozzle release experiments are seen to be predicted with good precision for all three release rates.

The experiments also included releases from a 4 mm nozzle. As small releases may lead to quite long simulation times, the grid embedding guidelines were not followed strictly. Furthermore, very small flammable clouds were expected for these releases. The reason for such insignificant clouds in this case was the small inventory and high momentum that caused fast mixing and dilution below the LFL. As the resulting gas cloud sizes were indeed found to be insignificant, these simulations were not rerun with a better grid. These simulations are therefore excluded from the validation work described in the current article.

In Fig. 5, the lateral distribution of concentration is shown for the experiments with release from the 100 and 21 mm nozzle and compared to blind predictions. The sampling time and location is also given. For the 100 mm nozzle (left figures), it was found that the concentration from the lowest release rate was somewhat underestimated. However, this may be a result of the grid resolution applied since the plume width is only 10–15 cm, and the grid resolution is 5 cm (no control volume in the middle of the release). For the intermediate leak rate (0.7 g/s) a much better correlation is seen. For the large leak rate the plume width is well predicted, but some over-prediction of concentration is observed.

The lowest release rate case was resimulated with a finer grid (three grid cells across the leak). No change in the plume width was seen while the centre-line concentration increased to 39–40% that agrees much better with the experimental value of 33–34%. Since the plume width for the 0.7 g/s is only marginally larger (25–30 cm), this case was also resimulated with the finer grid described above. Again, no change in the plume width was seen while the centre-line concentration increased to 57–58% which is somewhat larger than

the experimental value of 38%. However, the agreement with measured values offset from the centre-line is somewhat better. The results of the post-calculations for the 100 mm nozzle are also presented in Fig. 5 along with the blind calculations. The results from the post-calculations for the 100 mm nozzle are also included in the vertical concentration profiles presented in Fig. 4. It can be seen that the calculated concentrations in the post-simulations are generally higher than the calculated values in the blind simulations. The concentration in the post-calculations are higher than the observed values far away from the release while they agree better with the observed values close to the release.

For the 21 mm nozzle (right figures), it can be seen that the simulated lateral concentrations correspond well with the experimental recordings for all three release rates. Both the maximum concentration and plume width are predicted with good accuracy. Nonetheless, the lowest release rate case was repeated with a finer grid (three grid cells across the leak). However, the results were virtually unchanged since in this case the original grid cell size near the release (2 cm) is sufficient to resolve the plume width of about 20 cm (the post-calculation results for the 0.15 g/s case are also included in Fig. 5). In Fig. 6, a background oriented Schlieren (BOS) picture with numerical measurements added (21 mm nozzle, 3 g/s) is shown and compared to a predicted concentration profile. It can be seen that the measured concentrations and shape of plume correspond well to the predictions.

The results from the second geometrical configuration are presented next. Concentrations obtained in the experiments from releases from the two large nozzle sizes in the hood geometry are presented in Fig. 7. The sampling time and location is also given. For the 3.5 g/s release (100 mm nozzle), the lateral distribution of concentration from FLACS predictions corresponds well with experimental data both for 1.25 and 1.05 m elevations (see left pictures in Fig. 7). However, the experimental jet axis concentration is 23% whereas a value of more than 35% is predicted by FLACS. Also the results for the 0.7 g/s release compare quite well with experiment, while the concentrations resulting from the 0.14 g/s release are somewhat under-predicted. However, the experimental results for the 0.14 g/s case depict some peculiar behaviour (the concentrations remain almost constant between the sidewalls and the centre-line). In the simulations, the grid resolution was 5 cm, i.e. the slowest leak was resolved by a region 2 × 2 grid cells across. A result of this is that there is no grid cell exactly on the central axis of the jet. The 0.14 g/s and the 0.7 g/s were also resimulated for the hood geometry with a finer grid resolution. The results are also presented in Fig. 7. In this case, it can be seen that the lateral concentration profiles are virtually unchanged. This may be attributed to a larger plume width that is seen in this case and thus, the original grid resolution was likely sufficient in this case. One should also take into
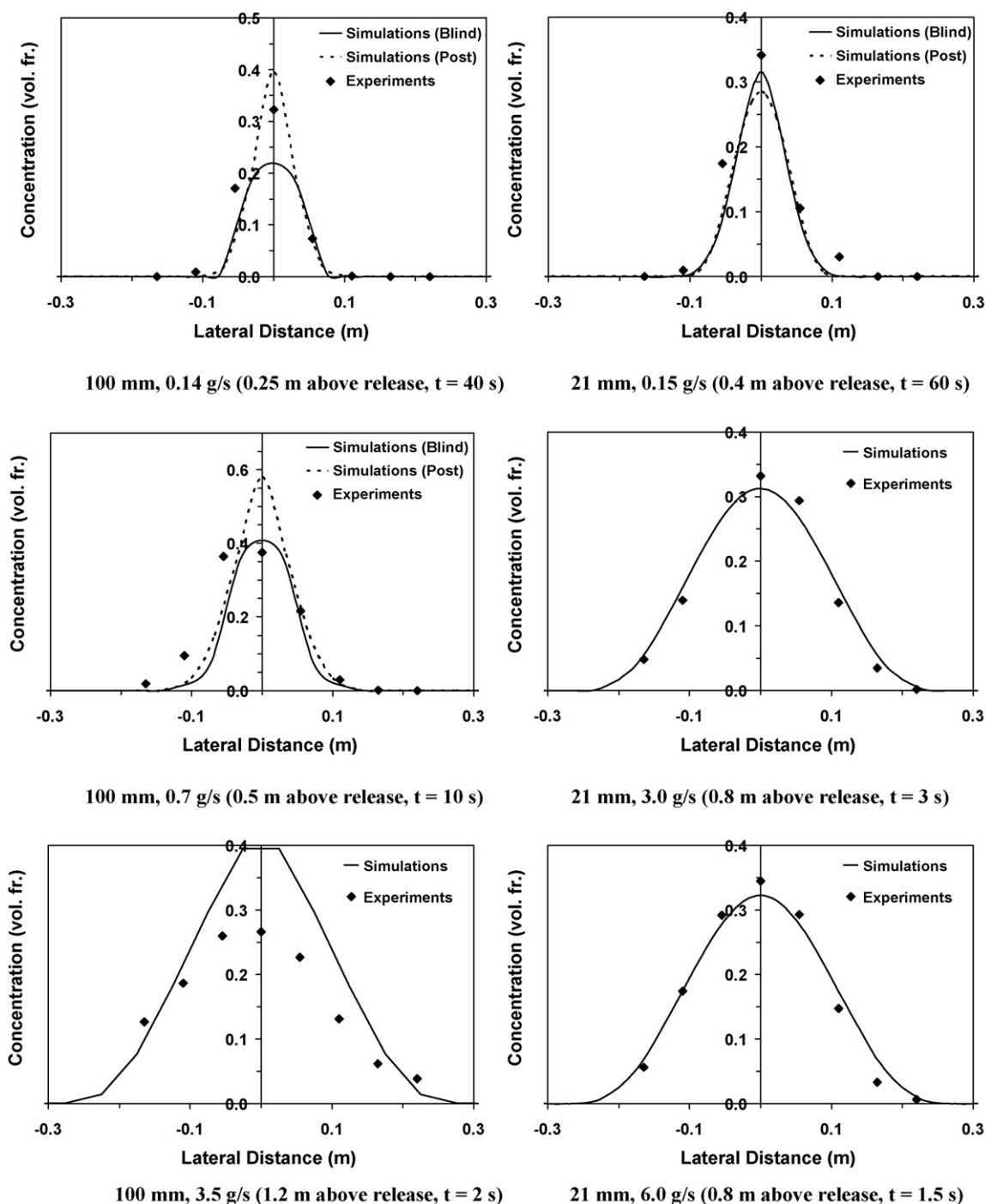
Fig. 5. Experimental horizontal concentration distribution vs. FLACS predicted results for releases from 100 and 21 mm nozzle in the FZK workshop geometry (plate only).

account that the experimental recordings have many uncertainties, as average concentrations will be approximated over a certain volume. This may also lead to deviations between predictions and observations in some cases.

The comparison of lateral concentrations resulting from releases from the 21 mm nozzle into the hood shows good correlation for the 3 g/s release, whereas the concentrations for the 0.15 g/s release are somewhat too low in simulations. Again, the lowest release rate has a much larger plume width in relation to simulations and the concentrations stay almost constant while a decay is seen in the simulations. It is again a question whether a better grid resolution across the jet will be required for such low momentum releases (for high momentum jet releases our approach with one grid cell

covering the leak seems to be sufficient, but for lower release velocities a finer grid may be required). This case was resimulated with a finer grid resolution (three grid cells across the leak). However, the change in the lateral concentration profile was insignificant (the results are also shown in Fig. 7). Again, this may be explained by the fact that the plume width is of the order of 30–40 cm in this case and the original grid resolution was 2 cm. Further, it is seen in general that the results are not changed significantly by using a finer grid for the 21 mm nozzle as compared to the observation for the 100 mm nozzle where a significant change was seen. One of the reasons could be that the exit velocity here is 5 m/s instead of 0.2 m/s. In Fig. 8, the experimental BOS picture with numerical measurements added (21 mm nozzle, 3 g/s) for the hood geometry
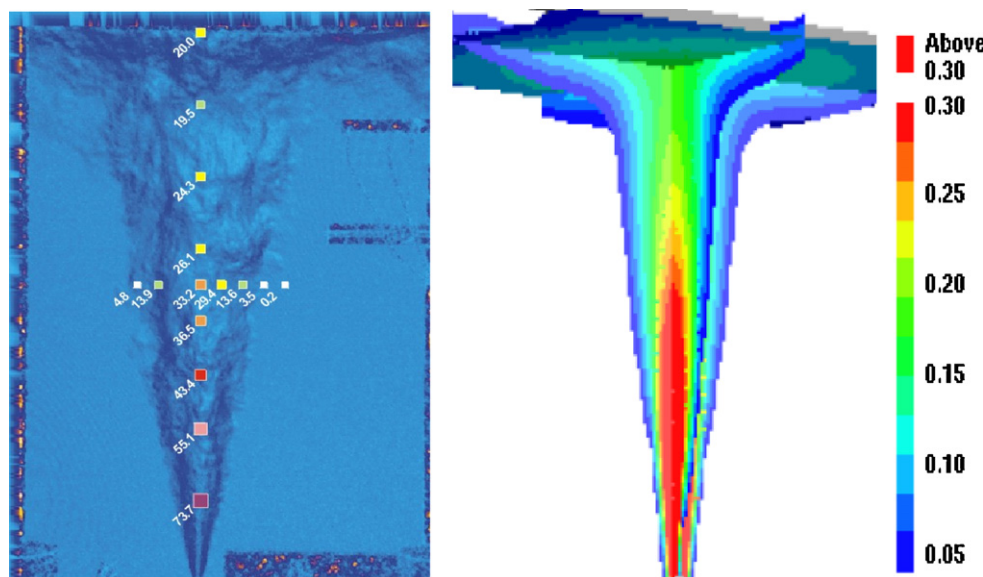
Fig. 6. Comparison of experimental photograph/recording with FLACS predicted plume shape and concentrations for release from 21 mm nozzle (3 g/s) towards plate.

is shown and compared to a predicted concentration profile. The measured concentrations and shape of plume correspond well to the predictions. In general, it can be seen that the shape of the plume is different for the hood geometry as compared to the plate geometry. The concentrations quickly approach zero in case of the plate geometry while significant concentration levels are maintained for the hood geometry, especially near the sidewalls.

4.2. Explosion

This section correlates experimental data and simulation predictions for overpressures obtained subsequent to ignition of dispersed clouds. A number of explosion simulations were performed in which the realistic gas clouds were ignited during the release. The results of the dispersion simulations were dumped at various times to be used as starting point for explosion calculations. All scenarios were ignited in the middle of the horizontal plate while some scenarios were also ignited at a location that is 0.63 m diagonally along the plate. As described above, a uniform grid of 2.5 cm grid cell size was applied to ensure a sufficient grid resolution inside the non-homogenous gas clouds. It must be noted that several of the explosion cases (0.7 and 3.5 g/s release rate for the 100 mm nozzle and 3 and 6 g/s release rates for the 21 mm nozzle, see Table 3) cannot be directly compared to the predictions performed with FLACS as experiments used flame accelerating obstacles whose dimensions cannot easily be described in detail. Further, for the experiments where these obstacles were not used, the ignition points in the simulations were somewhat different from those in the experiments. Still the observed pressure levels are comparable to those reported blind.

For the smallest release cases (0.14 g/s for the 100 mm nozzle and 0.15 g/s release rate for the 21 mm nozzle), very small values of overpressures (1–3 mbar) were predicted. This agrees very well with the observed values of 0.5–1.5 mbar. Due to a different ignition point used in the experiments compared to the initial simulations for the cases indicated above, we resimulated eight explosion tests again in order to be able to compare with experiments directly with the same ignition position and ignition time. Please note that all these simulations have been performed for realistic gas clouds obtained as a result of the hydrogen release. The calculated overpressures for the 0.7 g/s release rate for the 100 mm nozzle ranged from 4 to 6 mbar that again compares well with the observed values

of 2–4 mbar. The results for the other three cases are summarized in Fig. 9. Here, two different ignition positions (0.8 and 1.2 m above the release) were used. The results for the ignition position 0.8 m above the release nozzle are presented first. In this case, the simulated overpressures range from 5 to 15 mbar for the plate scenario and 10–40 mbar for the hood scenario. This corresponds reasonably well with the experimentally observed overpressures of 5–10 mbar for the plate scenario and 10–50 mbar for the hood scenario. The general pressure level (few mbar) is captured and the simulations lie generally on the conservative side. The results for the ignition position 1.2 m above the release location are also seen in Fig. 9. It can be seen that three of the FLACS simulations give explosion pressures of 5–30 mbar, which corresponds reasonably to the measured pressures of 5–20 mbar. For one of the cases (100 mm nozzle, hood geometry) for the higher ignition position, FLACS predicts a much higher pressure (30–50 mbar) than is seen in experiment (10 mbar). One possible reason for the general larger discrepancy with the higher ignition position is the fact that the concentrations near the ignition point are either quite rich (ER ∼ 1.7) or quite lean (ER ∼ 0.6) depending on the nozzle diameter while they are near stoichiometry for all cases for the lower ignition position. The precision level of the simulations is less for concentrations far away from stoichiometry and the burning rate is rather too high (Lewis number effects are quite dominant for concentrations far away from stoichiometry and they are only implemented approximately). However, the simulations lie on the conservative side and bound all the scenarios (this is very important for risk studies). Also, same trends are seen when comparing simulated and observed overpressure values.

The results of the comparison of explosion pressures between experiments and simulations are encouraging. It can be concluded that simulated explosion pressures when igniting releases correspond reasonably well to the experimental observations. This points to the ability of FLACS to model the combined phenomenon of dispersion and direct ignition of non-homogeneous clouds with jet-induced turbulence.

4.3. Equivalent stoichiometric gas cloud (Q9) representation

To get an indication of expected explosion severity following a release, it can be more useful to consider the flammable volume as function of time (Q0) and also the FLACS estimated equivalent stoichiometric gas cloud (Q9). The equivalent stoichiometric gas cloud
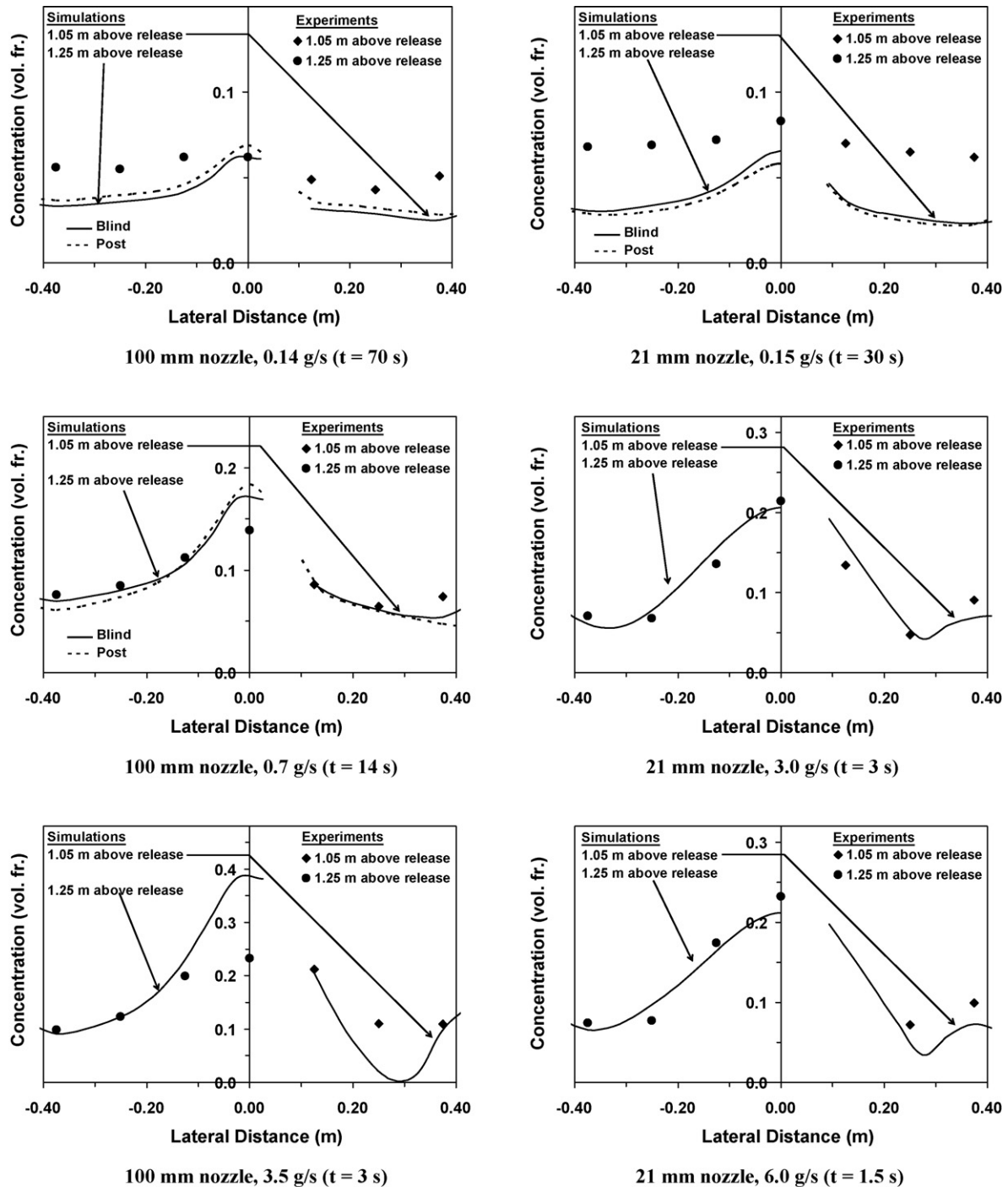
Fig. 7. Comparison of experimental and predicted horizontal concentration distribution for releases in the workshop geometry (hood geometry).

concept has been developed through our work towards quantitative risk assessment (QRA) for oil and gas applications. Herein, the dispersed gas clouds with non-homogenous distribution of gas and turbulence from jet are normally replaced by smaller equivalent stoichiometric gas clouds, Q9 [22]. Q9 cloud is a scaling of the non-homogeneous gas cloud to a smaller stoichiometric gas cloud that is expected to give similar explosion loads as the original cloud (provided conservative shape and position of cloud, and conservative ignition point). It is defined as $Q9 = \sum V \times BV \times E/(BV \times E)_{max}$. Here, V is the flammable volume, BV is the laminar burning velocity (corrected for flame wrinkling/Lewis number effects), E is volume expansion caused by burning at constant pressure in air, and the

summation is over all control volumes. The justification behind the applicability of the above concept is the fact that the combustion overpressures are broadly dependent on two main parameters, i.e. expansion and reactivity. Therefore, the potential overpressure contribution of the gas cloud of a given concentration can be evaluated by scaling these two parameters with respect to the maximum values (both these parameters go through a maximum as a function of concentration). As a practical guideline, it is recommended to choose the shape of the cloud that will give maximum travel distance from ignition to end of cloud for smaller clouds. For larger clouds, end ignition scenarios with longer flame travel should also be investigated. The Q9 concept is not meant to "bound" single
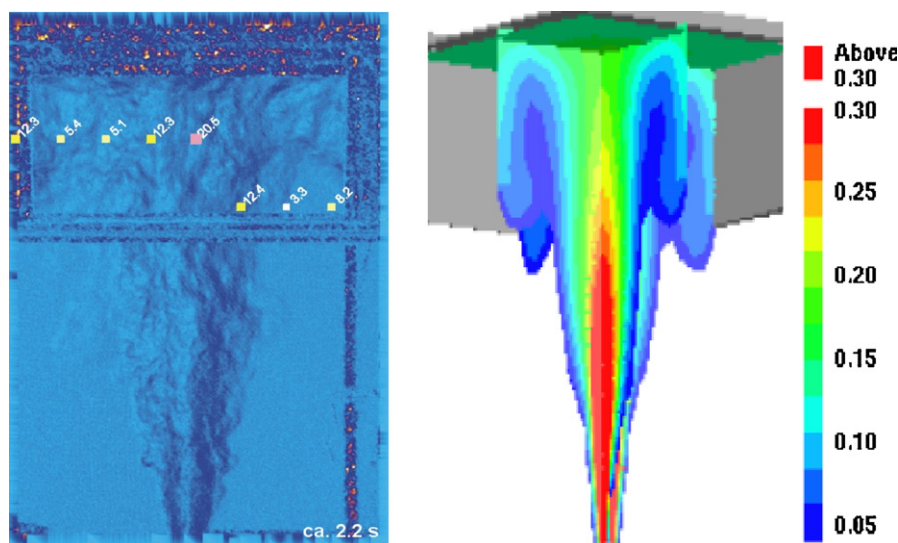
Fig. 8. Comparison of experimental photograph/recording with FLACS predicted plume shape and concentrations for release from 21 mm nozzle (3 g/s) in the hood geometry.

scenarios (for instance where experiments exist). This concept is useful for QRA studies with many simulations, and has been found to work reasonably well for safety studies involving natural gas releases in the Phase3B experiments performed at the Spadeadam test site [22]. The explosion loads are expressed as a function of cloud sizes and this approach can significantly reduce the number of dispersion and explosion calculations required to analyse the risk. Jet-induced turbulence should be considered if thought to be important. For a scenario of high confinement or a scenario where very high flame speeds are expected (not relevant in this case), only

Fig. 9. FZK experimental overpressures compared with FLACS simulated explosion overpressures of ignited jets for ignition location along the jet axis 0.8 m from release nozzle (top) and 1.2 m (bottom) from release nozzle.

expansion based weighting should be used. As one of the goals of this study is to develop corresponding risk assessment methods for hydrogen systems, we have investigated the applicability of this concept to the present system. More details are given below.

The size of the equivalent stoichiometric gas cloud as a function of time for the two scenarios shown in Figs. 6 and 8 is presented in the left plot of Fig. 10, where it can be seen that the hood geometry presents a greater risk as expected. In the right plot in Fig. 10, the maximum experimental pressures predicted by simulations for all different scenarios (plate and hood geometry) are summarized as a function of an "equivalent" stoichiometric gas cloud size Q9. The figure also includes a table containing the conditions of the performed simulations supporting the right plot in Fig. 10. The overpressure that is reported here is the maximum overpressure at a set of 30 monitor points (details are given in Section 3). This figure only includes blind simulations carried out prior to the experiments for two different ignition positions: center and edge. Three different ignition times were used for each dispersion scenario (chosen based on the time of maximum value of Q9) in order to obtain the "worst-case" explosion pressure (4 mm nozzle size was not considered since the gas cloud sizes were very insignificant). Even though these ignition positions and times did not have any direct correlation with those used in the experiments, the goal with this part of the study was to obtain worst-case overpressures and evaluate how they correlated with the gas cloud size. For the plate only geometry it can be seen that the maximum pressure is 40 mbar; however, the majority of predicted explosion pressures are in the range 0–20 mbar. Further, it must be pointed out that even if a pressure of 40 mbar was reported in the worst-case, the highest pressure was due to a short local initial pressure transient in connection to ignition, and the main pressure level is rather 20 mbar than 40 mbar. In the hood geometry, the maximum predicted pressure level reached 80 mbar, but most of the explosions produced pressures in the range 20–40 mbar (some were below 10 mbar). The lines indicate reference calculations using homogeneous stoichiometric gas clouds. In this plot, the solid line indicates the pressure level found in quiescent explosion scenarios with a conservative cloud location and ignition point (rectangular stoichiometric cloud located centrally towards the plate with ignition centrally on plate, but turbulence from jet ignored) for the hood geometry while the dashed line indicates the corresponding pressure level for the plate geometry. The reference calculations were performed using three gas cloud sizes: 13, 63 and 500 L.
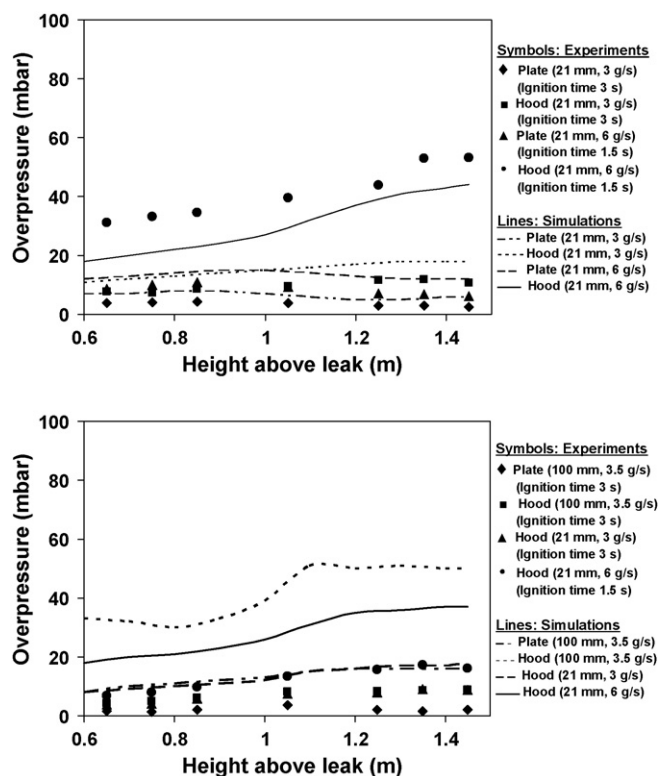
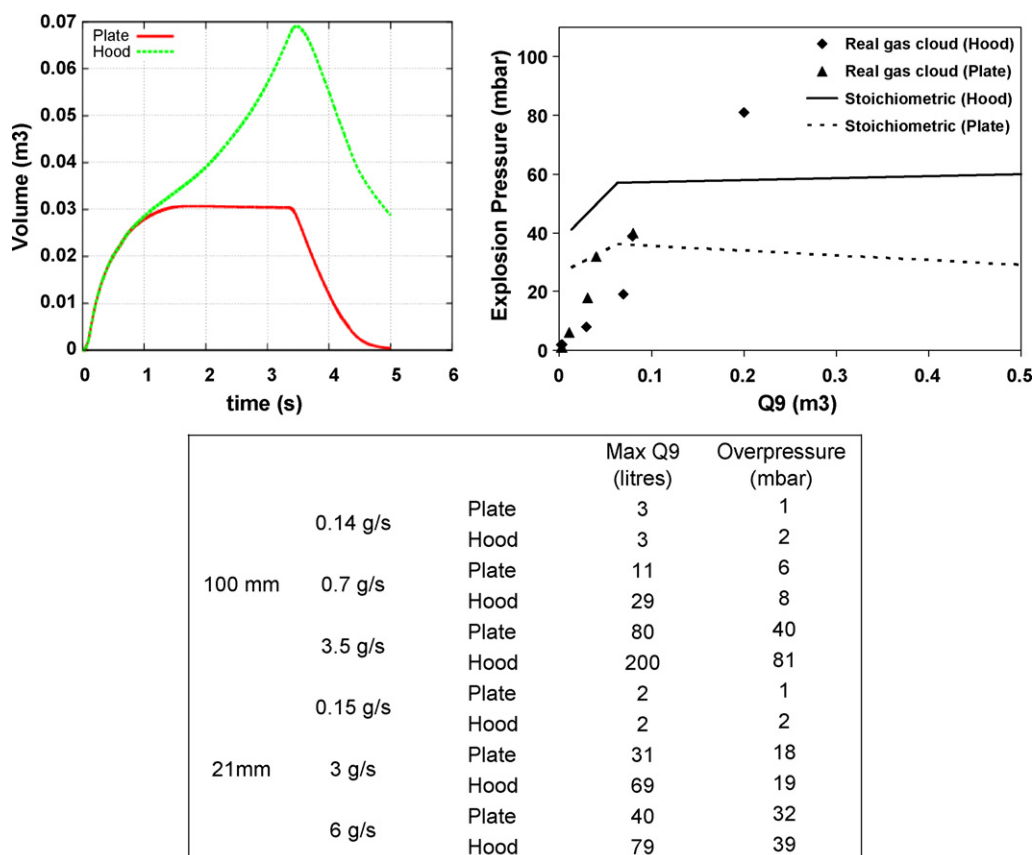|			Max Q9 (litres)	Overpressure (mbar)
100 mm	0.14 g/s	Plate	3	1
		Hood	3	2
	0.7 g/s	Plate	11	6
		Hood	29	8
	3.5 g/s	Plate	80	40
		Hood	200	81
21mm	0.15 g/s	Plate	2	1
		Hood	2	2
	3 g/s	Plate	31	18
		Hood	69	19
	6 g/s	Plate	40	32
		Hood	79	39

Fig. 10. (Left) Equivalent stoichiometric gas cloud as a function of time for the 21 mm release scenarios (3 g/s) for the plate and hood geometries (see Figs. 6 and 8). (Right) Blind predicted overpressures in hood (solid) and plate (dashed) configurations as function of estimated Q9 equivalent cloud size (FLACS QRA-method) for ignited leaks. Reference calculations with homogenous stoichiometric gas clouds are included. A table showing the conditions of the performed simulations is also included.

The plot shown in Fig. 10 supports the methodology of igniting idealized stoichiometric clouds to indicate the expected overpressure level. For the plate situation, the "dashed" line corresponds well with the simulated realistic pressures. However, for the hood situation one of the simulated explosions gives 30% higher pressure than the solid curve, but still the "solid" curve gives a representative pressure level for the situation with the hood. This can be explained by the fact that jet-induced turbulence is neglected while reference results using equivalent stoichiometric clouds are obtained. In some cases, jet-induced turbulence can cause the overpressures to go up by a factor of 2–3. Findings like those shown above are important for the development of risk assessment methods, as it is unrealistic to simulate 1000 s of ignition locations (variations in time and ignition location for a range of dispersion calculations). If the output from the dispersion calculations can be sorted into different homogenous cloud sizes based on the FLACS Q9 parameter, this can reduce required number of explosion simulations by orders of magnitude.

5. Conclusions

A number of CFD simulations of selected scenarios of impinging jet gas dispersion and subsequent gas explosion were performed with FLACS as predictions of experiments that were performed by FZK. Based on the comparison between observations and predictions, the following conclusions can be made:

1. In general the prediction of various scenarios of hydrogen release and dispersion were in good agreement with the results of the FZK experiments. Both the lateral and the vertical concentration profiles were compared with the experiments. The best predictions were obtained for the high momentum releases (21 mm nozzle) whereas somewhat lower precision was obtained for the low momentum release scenarios with 100 mm nozzle. However, the calculations were performed in a typical risk assessment project setting, in which many CFD calculations were simulated quickly (within 1–2 weeks). Nonetheless, the agreement between simulations and experiments is better than expected.
2. The explosion overpressures for the lowest release rates for both nozzles were very small (less than 5 mbar). These were predicted well by the blind simulations. The ignition points in several of the explosion scenarios used in the initial blind simulations deviated from those eventually chosen in the subsequent FZK experiments. Hence, no direct comparison of the simulated and actual explosion developments could be performed. After the experiments some ignition cases were resimulated with the same ignition locations that were used in the experiment, and for seven out of eight examples the simulated overpressures corresponded well to the experimental observations.
3. Post-calculations with a better grid were carried out for low momentum releases where the grid resolution could be insufficient in the blind calculations. Somewhat better agreement was seen for the 0.14 g/s case for the 100 mm nozzle but no change was seen for most of the cases, especially for the hood geometry. Thus, the grid resolution used in the initial study was sufficient in most cases.
4. The explosion pressures predicted by FLACS before the experiments were quite similar to those obtained in the experiments, both for ignition of non-homogeneous clouds during releases, but equally importantly, the explosion pressures from the esti-

mated equivalent gas clouds (Q9-method) also corresponded well with the observations in the experiments. Thus, our risk assessment approach, in which the reactivity of the dispersed cloud is translated into an equivalent stoichiometric smaller cloud size (without initial turbulence, but with conservative cloud position and shape, and ignition location), gives a good indication of expected overpressures.

It seems justified to conclude that the results reported in this paper gives further support to the view that available advanced CFD tools are in fact able to simulate combined scenarios of release of combustible gas, entrainment by air, and subsequent gas explosion. Validation of the computational tools against good experiments is crucial. Published experimental data from experiments of the kind conducted by FZK are very scarce, and therefore the availability of these data in the present investigation was decisive. However, the scale of the FZK experiments is comparatively small in relation to large industrial scales, and the resulting explosions correspondingly less severe. Hence, any future possibility of validating advanced computational tools like FLACS against results from this type of combined experiments in lager scales should indeed be welcomed.

Acknowledgements

References

[1] O.R. Hansen, J. Renoult, M.P. Sherman, S. Tieszen, Validation of FLACS-hydrogen CFD consequence prediction model against large scale H_2 explosion experiments in the FLAME facility, in: Proceedings of 1st International Conference on Hydrogen Safety, Pisa, Italy, September 2005, 2005.
[2] E. Gallego, E. Migoya, J.M. Martin-Valdepeñas, A. Crespo, J. García, A.G. Venetsanos, E. Papanikolaou, S. Kumar, E. Studer, Y. Dagba, T. Jordan, W. Jahn, S. Høiset, D. Makarov, J. Piechna, An inter-comparison exercise on the capabilities of CFD models to predict distribution and mixing of H_2 in a closed vessel, Int. J. Hydrogen Energy 32 (2007) 2235–2245.
[3] P. Middha, O.R. Hansen, M. Groethe, B.J. Arntzen, Hydrogen explosion study in a confined tube: FLACS CFD simulations and experiments, in: Proceedings of 21st International Colloquium of Dynamics of Explosions and Reactive Systems, Poitiers, France, July 23–27, 2007, 2007.
[4] P. Middha, O.R. Hansen, H. Schneider, Deflagration to detonation transition (DDT) in Jet ignited hydrogen-air mixtures: large scale experiments and FLACS CFD predictions, in: Proceedings of 12th International Symposium on Loss Prevention and Safety Promotion in the Process Industries, Edinburgh, UK, May 22–24, 2007, 2007.
[5] P. Middha, O.R. Hansen, I.E. Storvik, Prediction of deflagration to detonation transition in hydrogen explosions, in: Proceedings of the AIChE Spring National Meeting and 40th Annual Loss Prevention Symposium, Orlando, FL, April 23–27, 2006, 2006.
[6] P. Middha, O.R. Hansen, I.E. Storvik, Validation of CFD-model for hydrogen dispersion. Proceedings of the World Conference on Safety of Oil and Gas Industry (WCOGI) 2007, Gyongju, South Korea, April 10–13, 2007, J. Loss Prevent. Proc. Ind., 22 (2009) 1034–1038.
[7] A.G. Venetsanos, E. Papanikolaou, M. Delichatsios, J. Garcia, O.R. Hansen, M. Heitsch, A. Huser, W. Jahn, T. Jordan, J.-M. Lacome, H.S. Ledin, D. Makarov, P. Middha, E. Studer, A.V. Tchouvelev, A. Teodorczyk, F. Verbecke, M.M. Van der Voort, An inter-comparison exercise on the capabilities of CFD models to predict the short and long-term distribution and mixing of hydrogen in a garage, Proceedings of 2nd International Conference on Hydrogen Safety, San Sebastian, Spain, 11–13 September 2007, Intl. J. Hydrogen Energy 34 (2009) 5912–5923.
[8] T. Jordan, J. García, O.R. Hansen, A. Huser, S. Ledin, P. Middha, V. Molkov, J. Travis, A.G. Venetsanos, F. Verbecke, J. Xiao, Results of the HySafe CFD validation benchmark SBEP-V5, in: Proceedings of 2nd International Conference on Hydrogen Safety, San Sebastian, Spain, 11–13 September 2007, 2007.
[9] P. Middha, O.R. Hansen, CFD-based risk assessment for hydrogen applications, Proc. Saf. Prog. 27 (2008) 29–34.
[10] P. Middha, O.R. Hansen, Using computational fluid dynamics as a tool for hydrogen safety studies, J. Loss Prev. Proc. Ind. 22 (2009) 295–302.
[11] A. Friedrich, J. Grune, N. Kotchourko, A. Kotchourko, K. Sempert, G. Stern, M. Kuznetsov, Experimental study of jet-formed hydrogen-air mixtures and pressure loads from their deflagrations in low confined surroundings, in: Proceedings of 2nd International Conference on Hydrogen Safety, San Sebastian, Spain, 11–13 September 2007, 2007.
[12] B.H. Hjertager, Computer simulation of turbulent reactive gas dynamics, J. Model. Identification Control 5 (1985) 211–236.
[13] B.A. Arntzen, Modeling of turbulence and combustion for simulation of gas explosions in complex geometries, PhD Thesis, 1998, NTNU, Trondheim, Norway.
[14] B.H. Hjertager, K. Fuhre, M. Bjorkhaug, Gas explosion experiments in 1:33 and 1:5 scale offshore separator and compressor modules using stoichiometric homogeneous fuel/air clouds, J. Loss Prev. Proc. Ind. 1 (1988) 197–205.
[15] B.H. Hjertager, M. Bjørkhaug, K. Fuhre, Explosion propagation of non-homogeneous methane-air clouds inside an obstructed 50 m^3 vented vessel, J. Hazard. Mater. 19 (1988) 139–153.
[16] O.R. Hansen, I. Storvik, K. van Wingerden, Validation of CFD-models for gas explosions, where FLACS is used as example: model description and experiences and recommendations for model evaluation, in: Proceedings of the European Meeting on Chemical Industry and Environment III Krakow, Poland, 1999, pp. 365–382.
[17] http://www.gexcon.com/index.php?src=flacs/overview.html, Accessed 24th February, 2009.
[18] O.J. Taraldset, FLACS v9.0 Manual, GexCon R&D, 2009.
[19] R.G. Abdel-Gayed, D. Bradley, M. Lawes, Turbulent burning velocities: A general correlation in terms of straining rates, Proc. R. Soc. Lond. A 414 (1987) 389–413.
[20] K.N.C. Bray, Studies of the turbulent burning velocity, Proc. R. Soc. Lond. A 431 (1990) 315–335.
[21] O.R. Hansen, P. Middha, GexCon blind simulations compared to FZK experiments, Technical Note CMR-07-F46207-TN-1, Bergen, Norway, January 19, 2007 (available to HySafe partners).
[22] NORSOK Standard Z-013, Risk and emergency preparedness analysis. Rev. 2. September 2001, available from http://www.nts.no/norsok.